MOMENTUM DISTRIBUTION FUNCTIONS
OF WEAKLY-DEGENERATE HYDROGEN PLASMA

A. S. LARKIN[1,2] AND V. S. FILINOV[1]

[1] Joint Institute for High Temperatures of the Russian Academy of Sciences
Izhorskaya 13 Bldg 2, 125412 Moscow, Russia
e-mail: alexanderlarkin@rambler.ru

[2] Moscow Institute of Physics and Technology
Institutskiy Pereulok 9, 141700 Dolgoprudny, Moscow Region, Russia

Summary. Quantum effects may change form of equilibrium momentum distribution function making it non-maxwellian due to Heisenberg uncertainty principle in scattering. In strongly coupled Coulomb systems "quantum tails" at high momenta are expected. In this paper, equilibrium momentum distributions in non-degenerate hydrogen plasma were calculated numerically. It was shown that electronic distributions have "quantum tails" when protons are maxwellian.

1 INTRODUCTION

It is well known that in classical statistics momenta of interacting particles at thermodynamical equilibrium have Maxwellian distribution. Quantum effects may change the equilibrium distributions of momenta, making them non-maxwellian. For instance exchange effects in electronic systems leads to Fermi–Dirac distribution instead of maxwellian. However even without exchange the distribution function of interacting particles can be non-maxwellian due to Heisenberg uncertainty principle in scattering of particles.

For a Coulomb system in [1] it was shown that momentum distribution takes "quantum tail" with power law $1/p^8$. Later this problem was studied in [2–5] where the form of "quantum tail" was corrected. Such quantum effects may play a big role in the study of combustion, detonation, vibration relaxation, chemical reactions and even low-temperature nuclear fusion. They are also important in the study of kinetic properties of many-particle systems. However under corresponding conditions particles usually are strongly coupled and perturbative methods can not be applied. Therefore for studies of momentum distributions in such systems numerical ab initio approaches are required.

Computer simulation is one of the main tools in studies of thermodynamic properties of many-particle strongly coupled Coulomb systems. Some of the most powerful numerical methods for simulation of quantum systems are Monte Carlo methods, based on path integral (PIMC) formulation of quantum mechanics [6]. This methods use path integral representation for partition function and thermodynamic values such as average energy, pressure, heat capacitance etc. PIMC methods are widely used for studying dense hydrogen plasma [7], electron gas in

metal [8–10], electron–hole plasma [11] in semiconductors, superfluidity [12–14] and even quark–gluon plasma [15–17].

Unfortunately usual PIMC methods cannot cope with problem of calculation of average values of arbitrary quantum operators in phase space or momentum distribution function, while this problem may be central in studies of kinetic properties of matter. The Wigner formulation of quantum mechanics in phase space allows more naturally to consider not only thermodynamical values but also kinetic properties. Methods for phase space treatment of the single-particle quantum dynamics in Wigner approach in microcanonical ensemble were proposed in [18–22]. Recently a generalization of these virtual particle one-body Wigner Monte Carlo methods to the many-body distinguishable particles has been done in [23]. Wigner dynamics of a relativistic particle was studied in [24].

In this paper we apply the *ab initio* phase space Monte Carlo approach developed in [25, 26] to non-degenerate hydrogen plasma. We calculated momentum distribution functions of electronic and protonic components for strongly coupled ($\Gamma \approx 1$) plasma. Preliminary results for "quantum tails" in electronic distribution was obtained.

2 WIGNER FUNCTION OF COULOMB SYSTEM

In this paper we consider a two-component system of charged particles with Coulomb interaction. Hamiltonian is

$$
\begin{aligned}
H(p,q) = \sum_{a=1}^{N} \frac{\mathbf{p}_{ea}^2}{2m_e} + \sum_{a=1}^{N} \frac{\mathbf{p}_{ha}^2}{2m_p} + \sum_{a=1}^{N}\sum_{b=a+1}^{N} \frac{(-e)(-e)}{|\mathbf{q}_{ea}-\mathbf{q}_{eb}|} + \sum_{a=1}^{N}\sum_{b=a}^{N} \frac{(-e)(+e)}{|\mathbf{q}_{ea}-\mathbf{q}_{pb}|} \\
+ \sum_{a=1}^{N}\sum_{b=a+1}^{N} \frac{(+e)(+e)}{|\mathbf{q}_{pa}-\mathbf{q}_{pb}|},
\end{aligned}
\tag{1}
$$

where p_{ea} and q_{ea} are momentum and position of a-th particle with mass m_e and electrical charge $-e$, and p_{ha} and q_{ha}—the same for a-th particle with mass m_p and electrical charge $+e$. We will call the negative-charged particles as "electron" and the positive-charged particles as "proton" meaning applications to hydrogen plasma. Numbers of electrons N_e and protons N_p we consider equal ($N_e = N_p = N$) so system is quasineutral.

We focus on canonical ensemble of system (1) with fixed numbers of particles N, volume V and temperature T. Density matrix in q-representation in this case is

$$
\rho(q,q';\beta) = \langle q|e^{-\beta\hat{H}}|q'\rangle,
\tag{2}
$$

where $\beta = 1/kT$ is reciprocal temperature, and $|q\rangle$ is quantum state of N particles with determined positions. We will consider a non-degenerate system, when states $|q\rangle$ and density matrix

(2) are not (anti)symmetrized. In fact, we consider Boltzmann statistics instead of Fermi–Dirac (Bose–Einstein) statistics. It is reasonable when $n_e \lambda_e^3 \leqslant 1$, $n_p \lambda_p^3 \leqslant 1$ i.e. average distance between particles $n_e^{-1/3}$ is less than De Broglie thermal wavelength

$$\lambda_e = \sqrt{\frac{2\pi\hbar^2}{mkT}}.$$

Herein we do not taking into account quantum exchange effects, only quantum interference and nonlocality.

2.1 Wigner function: path integral representation

An average value of some operator $\hat{A}$ can be written as a Weyl symbol $A(p,q)$, averaged over phase space of $2N$ particles with the Wigner function $W(p,q;\beta,V)$ [27]:

$$\langle\hat{A}\rangle = \int \frac{\mathrm{d}^{6N}p\,\mathrm{d}^{6N}q}{(2\pi\hbar)^{6N}} A(p,q) W(p,q;\beta,V). \tag{3}$$

Here we use a symbol p for momenta of $2N$ particles: $p = (\mathbf{p}_{e1},\ldots,\mathbf{p}_{eN},\mathbf{p}_{p1},\ldots,\mathbf{p}_{pN})$. So we deal with other variables. Here the Weyl symbol of operator $\hat{A}$ is:

$$A(p,q) = \int \frac{\mathrm{d}^{6N}s}{(2\pi\hbar)^{6N}} e^{isq/\hbar} \langle p+s/2|\hat{A}|p-s2\rangle. \tag{4}$$

Weyl symbols for common operators like $\hat{\mathbf{p}}$, $\hat{\mathbf{q}}$, $\hat{H}$, etc can be easily calculated directly from definition (4). The Wigner function of the $2N$-particle system in canonical ensemble is defined as a Fourier transform of the off-diagonal element of density matrix (2) in q-representation:

$$W(p,q;\beta,V) = Z(\beta,V)^{-1} \int \mathrm{d}^{6N}\xi\, e^{i\langle p,\xi\rangle/\hbar} \rho(q-\xi/2,q+\xi/2;\beta), \tag{5}$$

where $Z(\beta,V)$ is partition function of canonical ensemble of N particles and designation $\langle p,q\rangle = \sum_{a=1}^{N}(\mathbf{p}_{ea}\mathbf{q}_{ea} + \mathbf{p}_{pa}\mathbf{q}_{pa})$ is the sum over all particles. The Wigner function $W(p,q;\beta,V)$ corresponds to the classical distribution function in the phase space, and the Weyl symbol—to the classical observing quantity.

Since operators of kinetic and potential energy in Hamiltonian (1) do not commutate, the exact explicit analytical expression for Wigner function does not in exist. To overcome this difficulty we represent the Wigner function similarly to path integral representation of the partition function [6,28]. Exactly we represent the statistical operator $e^{-\beta\hat{H}}$ as a product of large number (M) of high-temperature operators $e^{-\varepsilon\hat{H}}$ and write the Wigner function in the form of a multiple

integral of the product of the high temperature density matrices:

$$W(p,q;\beta,V) = Z(\beta,V)^{-1} \int \mathrm{d}^{6N}\xi\, e^{i\langle p,\xi\rangle/\hbar} \int \mathrm{d}^{6N}q^1\dots\mathrm{d}^{6N}q^{M-1}$$

$$\times \left[\prod_{m=0}^{M-1}\langle q^m|e^{-\varepsilon\hat{H}}|q^{m+1}\rangle\right]\Bigg|_{q^0=q-\xi/2}^{q^M=q+\xi/2}. \tag{6}$$

If $\varepsilon \to 0$ the high temperature density matrices can be calculated with accuracy up to $O(\varepsilon^2)$ [6]:

$$\langle q^m|e^{-\varepsilon\hat{H}}|q^{m+1}\rangle \approx \lambda_\varepsilon^{-1} \exp\left[-\pi\lambda_\varepsilon^{-2}\langle q^{m+1}-q^m\rangle^2 - \varepsilon U(q^m;\varepsilon)\right], \tag{7}$$

where we use designation $\langle q^{m+1}-q^m\rangle^2 = \sum_{a=1}^N[(\mathbf{q}_{\mathrm{ea}}^{m+1}-\mathbf{q}_{\mathrm{ea}}^m)^2 + (\mathbf{q}_{\mathrm{pa}}^{m+1}-\mathbf{q}_{\mathrm{pa}}^m)^2]$, and λ_ε is the De Broglie thermal wavelength at high temperature MT,

$$\lambda_\varepsilon = \sqrt{\frac{2\pi\hbar^2\varepsilon}{m}}.$$

Also here the Kelbg pseudopotential is introduced instead of Coulomb potential [29]:

$$U(q;\varepsilon) = \sum_{a=1}^N\sum_{b=a+1}^N \frac{(-e)(-e)}{|\mathbf{q}_{\mathrm{ea}}-\mathbf{q}_{\mathrm{eb}}|}\phi_\varepsilon(\mathbf{q}_{\mathrm{ea}}-\mathbf{q}_{\mathrm{eb}}) + \sum_{a=1}^N\sum_{b=a}^N \frac{(-e)(+e)}{|\mathbf{q}_{\mathrm{ea}}-\mathbf{q}_{\mathrm{pb}}|}\phi_\varepsilon(\mathbf{q}_{\mathrm{ea}}-\mathbf{q}_{\mathrm{pb}})$$

$$+ \sum_{a=1}^N\sum_{b=a+1}^N \frac{(+e)(+e)}{|\mathbf{q}_{\mathrm{pa}}-\mathbf{q}_{\mathrm{pb}}|}\phi_\varepsilon(\mathbf{q}_{\mathrm{pa}}-\mathbf{q}_{\mathrm{pb}}), \tag{8}$$

$$\phi(r_{\mathrm{ab}})_\beta = 1 - e^{-r_{\mathrm{ab}}^2/\lambda_{\varepsilon ab}^2} + \sqrt{\pi}\frac{r_{\mathrm{ab}}}{\lambda_{\varepsilon ab}}[1 - erf(r_{\mathrm{ab}}/\lambda_{\varepsilon ab})] \tag{9}$$

where $\lambda_{\varepsilon ab}^2 = \frac{\hbar^2\beta}{2\mu_{\mathrm{ab}}}$, $\mu_{\mathrm{ab}}^{-1} = m_a^{-1} + m_b^{-1}$.

Thus expression for Wigner function takes the form:

$$W(p,q;\beta,V) = Z(\beta,V)^{-1} \int \mathrm{d}^{6N}\xi\, e^{i\langle p,\xi\rangle/\hbar} \int \mathrm{d}^{6N}q^1\dots\mathrm{d}^{6N}q^{M-1}$$

$$\times \exp\left\{-\frac{1}{M}\sum_{m=0}^{M-1}\left[\pi\frac{M^2}{\lambda^2}\langle q^{m+1}-q^m\rangle^2 + \beta U(q^m)\right]\right\}\Bigg|_{q_0=q-\xi/2}^{q_M=q+\xi/2}, \tag{10}$$

where $\lambda = \sqrt{2\pi\hbar^2\beta/m}$ is the thermal wavelength at temperature T.

In continuous limit $M \to \infty$ expression (10) turns into path integral over trajectories $q(\tau)$ starting at point $q - \xi/2$ and ending at $q + \xi/2$, where τ is a dimensionless parameter that can

be interpreted as "imaginary time" [6]:

$$W(p,q;\beta,V) = Z(\beta,V)^{-1} \int d^{6N}\xi\, e^{i\langle p,\xi\rangle/\hbar} \int_{q(0)=q-\xi/2}^{q(1)=q+\xi/2} D^{6N}q(\tau)$$

$$\times \exp\left\{-\pi \int_0^1 d\tau \left[\frac{\langle \dot{q}(\tau)\rangle^2}{\lambda^2} + \frac{\beta}{\pi}U\left(q(\tau)\right)\right]\right\}. \tag{11}$$

Measure of path integral (11) depends on Fourier variables ξ and positions q. To avoid this we change variables from trajectories $q(\tau)$ to closed dimensionless trajectories $z(\tau)$:

$$q(\tau) = \lambda z(\tau) + (1-\tau)(q-\xi/2) + \tau(q+\xi/2). \tag{12}$$

Taking into account the new boundary conditions $z(0) = z(1) = 0$ we obtain the path integral representation of Wigner function:

$$W(p,q;\beta,V) = Z(\beta,V)^{-1} \int d^{6N}\xi\, e^{i\langle p,\xi\rangle/\hbar} \sum_P (\pm 1)^P e^{-\frac{\pi}{\lambda^2}\langle \xi\rangle^2}$$

$$\times \int_{z(0)=z(1)=0} D^{6N}z(\tau) e^{-\pi \int_0^1 d\tau \left[\langle \dot{z}\rangle^2(\tau) + \frac{\beta}{\pi}U(q(\tau))\right]}, \tag{13}$$

where $q(\tau)$ is given by (12).

2.2 Harmonic approximation

Momenta p in expression (13) for the Wigner function are connected with other variables through $6N$-dimensional Fourier transform, which is not integrable analytically or numerically in general case. Exclusions are only linear or harmonic potentials, when order of variable $\bar{\xi}$ is less than two. In harmonic approximation we expand potential energy into Taylor series up to second order in $\bar{\xi}$:

$$U\left(\lambda z(\tau)+q+\xi(\tau-1/2)\right) \approx U\left(\lambda z(\tau)+q\right) + (\tau-1/2)\xi_{a,i}\frac{\partial U\left(\lambda z(\tau)+q\right)}{\partial q_{a,i}}$$

$$+\frac{1}{2}(\tau-1/2)^2\xi_{a,i}\xi_{b,j}\frac{\partial^2 U\left(\lambda z(\tau)+q\right)}{\partial q_{a,i}\partial q_{b,j}}, \tag{14}$$

where we mean summation over repeated indices a,b over all particles from 1 to $2N$ and i,j over dimensions from 1 to 3.

After that the expression for Wigner function (13) takes form of generalized gaussian integral over variable $\bar{\xi}$. Finally, harmonic approximation for the Wigner function can be written in the

following form:

$$W(p,q;\beta,V) = Z(\beta,V)^{-1} \int_{z(0)=z(1)=0} D^{6N} z(\tau) \exp\left\{-\pi K[z(\tau)] - \pi P[q,z(\tau)]\right\}$$

$$\times \exp\left\{-\frac{\lambda^2}{4\pi\hbar^2} p_{a,i} \chi_{ai,bj}[q,z(\tau)] p_{b,j} + \pi J_{a,i}[q,z(\tau)] \chi_{ai,bj}[q,z(\tau)] J_{b,j}[q,z(\tau)]\right\}$$

$$\times \det\left|\chi_{ai,bj}[q,z(\tau)]\right|^{1/2} \cos\left\{\frac{\lambda}{\hbar} p_{a,i} \chi_{ai,bj}[q,z(\tau)] J_{b,j}[q,z(\tau)]\right\}. \tag{15}$$

Here we introduced scalar functionals K and P, $6N$-vector functional $J_{a,i}$ and matrix functional $\chi_{ai,bj}$. They depends on trajectories $z(\tau)$ and positions q:

$$K[z(\tau)] = \int_0^1 d\tau \dot{z}^2(\tau),$$

$$P[q,z(\tau)] = \frac{\beta}{\pi} \int_0^1 d\tau U(q + \lambda z(\tau)),$$

$$J_{a,i}[q,z(\tau)] = \frac{\beta\lambda}{2\pi} \int_0^1 d\tau(\tau - 1/2) \frac{\partial U}{\partial q_{a,i}}(q + \lambda z(\tau)),$$

$$\chi_{ai,bj}[q,z(\tau)] = \left[\delta_{ab}\delta_{ij} + \frac{\beta\lambda^2}{2\pi} \int_0^\beta d\tau(\tau - 1/2)^2 \frac{\partial^2 U}{\partial q_{a,i} \partial q_{b,j}}\right]^{-1}.$$

Note that the first term in exponent (15) looks similarly to Maxwell distribution in classical statistics. The main differences are matrix $\chi_{ai,bj}[q,z(\tau)]$ and cosine. This matrix and cosine provide correlation of particle momenta with each other and with their positions and turn into units in case of non-interacting particles.

The expression for Wigner function (15) is obtained under assumption that potential energy U is expandable in Taylor series of second order ξ with a good accuracy. Note that the exponent (13) contains variable ξ in three places. The first one is in the Fourier term ($ip\xi/\hbar$), which makes momenta correlated with other dynamical variables. The second one is in the gaussian-like term ($-\pi\xi^2/\lambda^2$). The third one is in the integral term, where ξ is argument of potential:

$$\int_0^1 d\tau \beta U(q + \lambda z(\tau) + \xi(\tau - 1/2)).$$

The gaussian term provides fast decaying when ξ increases, so the main contribution comes from ξ near $\pi^{-1/2} \approx 0.6$. Argument of potential function contains $\bar{\xi}$ multiplied by $\tau - 1/2$, which is modulo less than 0.5. Using the mean value theorem, we can roughly get symbolic

estimation of these integrals in exponent (13) as

$$\frac{1}{n!}\frac{\partial^n U(q_0)}{\partial q^n}\int\limits_0^1 \mathrm{d}\tau\left(\tau-\frac{1}{2}\right)^n = \frac{1}{n!}\frac{(1+(-1)^n)}{(n+1)2^{n+1}}\frac{\partial^n U(q_0)}{\partial q^n}, \tag{16}$$

where x_0 is a certain point of trajectory. Numerical value of this integral rapidly decreases: when $n = 2, 4, 6$ it equals $1/24$, $1/1920$ and $1/322560$ correspondingly. Thus we expect negligible contribution of high order Taylor terms in potential expansion. Numerical calculations for some model of non-trivial potentials, done in [25, 26], confirm this assumption.

2.3 Monte-Carlo method

For calculation of $\langle\hat{A}\rangle$ in harmonic approximation (15) we use Monte Carlo method (MC) from [25, 26], generalized on two-component system of many particles in three spatial dimensions. Foremost one has to represent path integrals in discrete form of multiple integrals like (10). As a result we obtain expressions for MC calculations in the following form:

$$\langle\hat{A}\rangle = \frac{\left\langle A(p,q)f(p,q,z^1,\ldots,z^{M-1})h(p,q,z^1,\ldots,z^{M-1})\right\rangle_w}{\left\langle f(p,q,z^1,\ldots,z^{M-1})h(p,q,z^1,\ldots,z^{M-1})\right\rangle_w}. \tag{17}$$

Here brackets $\left\langle g(p,q,z^1,\ldots,z^{M-1})\right\rangle_w$ denote averaging of any function $g(p,q,z^1,\ldots,z^{M-1})$ with a positive weight $w(p,q,z^1,\ldots,z^{M-1})$:

$$\left\langle g(p,q,z^1,\ldots,z^{M-1})\right\rangle_w = \int \mathrm{d}^{3N}p\,\mathrm{d}^{3N}q\int \mathrm{d}z^1\ldots\mathrm{d}z^{M-1}g(p,q,z^1,\ldots,z^{M-1})$$
$$\times w(p,q,z^1,\ldots,z^{M-1}), \tag{18}$$

while

$$w(p,q,z^1,\ldots,z^{M-1}) = \exp\left\{-\frac{\lambda^2}{4\pi\hbar^2}p_{a,i}\chi_{ai,bj}p_{b,j} + \pi J_{a,i}\chi_{ai,bj}J_{b,j} - \pi K - \pi P\right\},$$
$$f(p,q,z^1,\ldots,z^{M-1}) = \cos\left\{\frac{\lambda}{\hbar}p_{a,i}\chi_{ai,bj}J_{b,j}\right\},$$
$$h(p,q,z^1,\ldots,z^{M-1}) = \det\left|\chi_{ai,bj}\right|^{1/2}. \tag{19}$$

To construct Metropolis algorithm we introduce three types of MC steps:

1. Variation of momentum of some particle: $\mathbf{p}_a \to \mathbf{p}_a + \delta\mathbf{p}_a$.

2. Variation of overall position of some particle: $\mathbf{q}_a \to \mathbf{q}_a + \delta\mathbf{q}_a$.

3. Variation of trajectory representing some particle: $\mathbf{z}_a^m \to \mathbf{z}_a^m + \delta\mathbf{z}_a^m$.

In our calculations probability of the first-type step is 0.1. Probability of the second-type step is also 0.1. Probability of the third-type step is 0.8, because each trajectory is represented by several dozens of variables z^m. Such choice allows the algorithm to find an "equilibrium" configuration much faster than choice of equal probabilities of each type of step. Acceptance probability of the steps is defined by positive function $w(p, q, z^1, \ldots, z^{M-1})$ according to standard Metropolis procedure. I.e. we calculate w for old configuration C, for probe configuration C'. Then aceptance probability is $min(1, w(C')/w(C))$. The first thousands of steps should be rejected during the calculation to "forget" initial configuration. We also use periodic boundary conditions only for overall positions q while trajectories $q(\tau)$ representing particles are able to leave the periodical cell.

3   NUMERICAL RESULTS

In this section, we present and discuss some numerical results, obtained by the developed Monte Carlo method for the Wigner function. We have been applied it to a two-component non-degenerate Coulomb system with fixed number of particles and temperature. Particles of the first type are of negative charge $-e$ and mass m_e, particles of the second type are of positive charge $+e$ and greater mass m_p. When m_e is electron mass and $m_p = 1836 m_e$ then this system is a model of hydrogen plasma. Let us consider specific thermodynamical parameters of the system.

Firstly, temperature T characterizes average kinetic energy of particles in equilibrium till system is non-degenerate. It means that Fermi energy of the electronic subsystem e_F should be much less than temperature: $kT \ll E_F$. This criterion of non-degeneracy may be rewritten in a convenient form:

$$n_e \lambda_e^3 \ll 1, \tag{20}$$

where n_e is electronic partial density, λ_e—De Broglie wavelength at temperature T. I.e. average distance between particles is much greater than De Broglie wavelength. In this case system of particles obeys Boltzmann statistics rather than Fermi–Dirac.

Secondly, the relation between temperature and average energy of interaction characterizes non-ideality of the system. Convenient parameter is so-called coupling strength:

$$\Gamma = e^2/(kTd), \qquad d = [3/(4\pi n_e)]^{1/3}, \tag{21}$$

with Wigner–Seitz radius d being average distance between electrons. We use Brueckner parameter $r_s = d/a_B$. When parameter $\Gamma \ll 1$ then Coulomb plasma is almost ideal. In other case it is strongly coupled and interaction can not be considered as a perturbation.
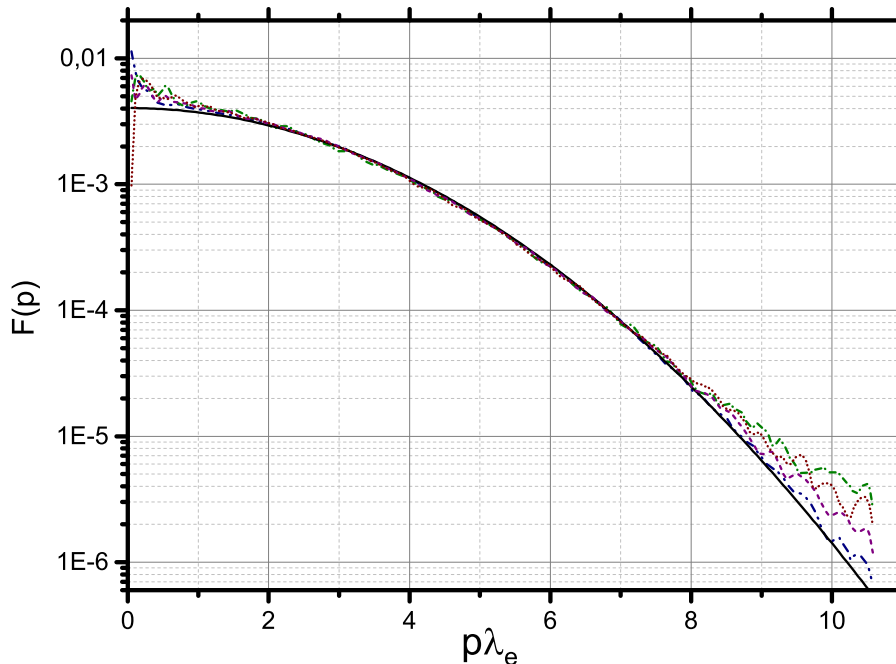
Figure 1: Momentum distributions of electrons in non-degenerate hydrogen plasma. Solid line refers to maxwellian distribution. Other lines from bottom to top correspond to $\Gamma = 0.4, 0.9, 1.1$ and 1.2. Corresponding temperatures are given in text. All distribution functions are normalized to unit area under the curves.

In this paper, we consider the range of Γ from 0.4 up to 1.2 for low densities to avoid the violation of condition $n_e \lambda_e^3 \leqslant 0.3$. In this case usage of Boltzmann statistics is quite justified. Consideration of such effects will lead to additional deformation of momentum distribution into Fermi function. However they does not have essential influence on expected quantum "tails" due to the uncertainty principle.

Under these conditions (weak degeneracy and moderate coupling strength) it is able to use the following set of parameters. Number of particles was taken $N_e = N_p = 10$, number of "inner quantum coordinates" $M = 20$, number of Monte Carlo steps—5×10^7. Increase of these parameters leads to great increase in the calculation time but does not affect on results significantly.

Momentum distribution functions for electronic component of hydrogen plasma are presented in figures 1 and 2. The black solid line shows the maxwellian distribution. Other lines refers to equilibrium distributions for non-ideal hydrogen plasma with coupling strength $\Gamma = 0.4, 0.9, 1.1, 1.2$ at fixed $n_e \lambda^3 = 0.3$. Corresponding temperatures kT are 1.16, 0.23, 0.15, 0.13 Ha while Brueckner parameters r_s are 2.16, 4.87, 5.94 and 6.47. Meaning parts of all distributions in $p\lambda_e/\hbar$ units are the same. However "quantum tails" at high momentum values appear. With increasing of non-ideality Γ the "tail" becomes more distinct. For instance when $\Gamma = 1.2$ electronic momentum distribution at $p = 10\hbar/\lambda_e$ is four times larger than maxwellian one.
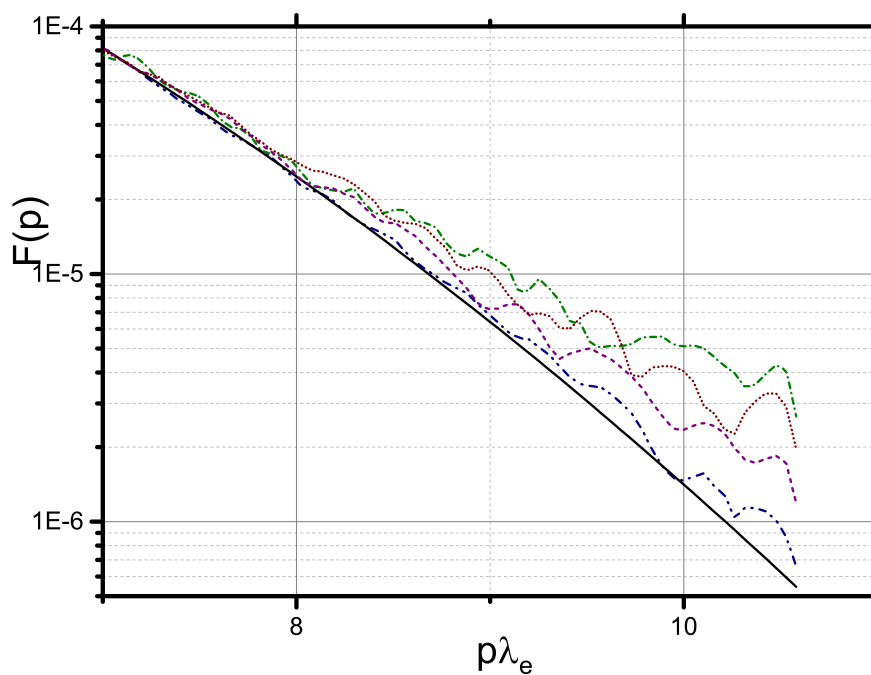
Figure 2: The same as in figure 1 but at high values of $p\lambda_e$ (in units of $\hbar$).
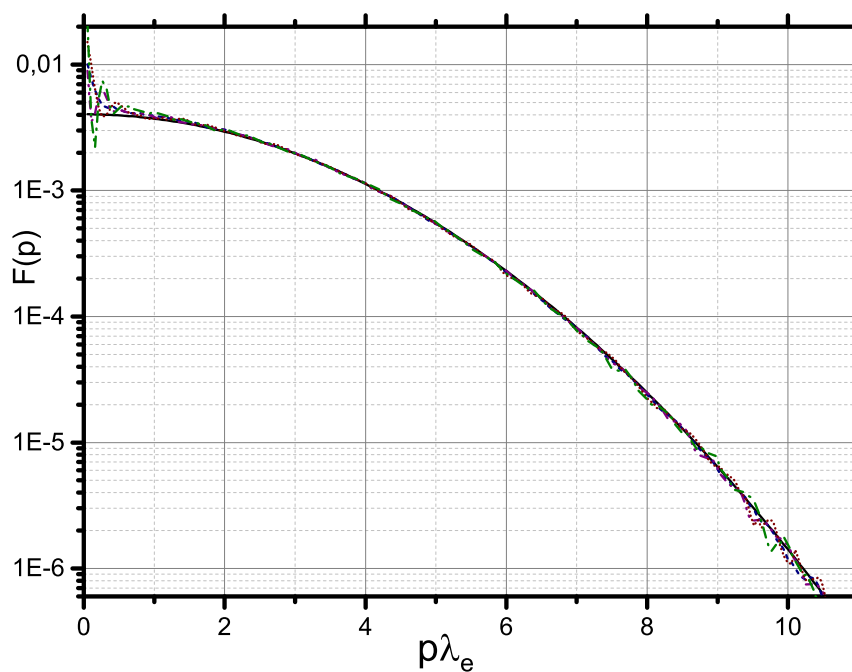

Figure 3: Momentum distributions of protons in non-degenerate hydrogen plasma. Solid line refers to maxwellian distribution. Other lines from bottom to top correspond to $\Gamma = 0.4, 0.9, 1.1$ and 1.2. Corresponding temperatures are given in text. All distribution functions are normalized to unit area under the curves.
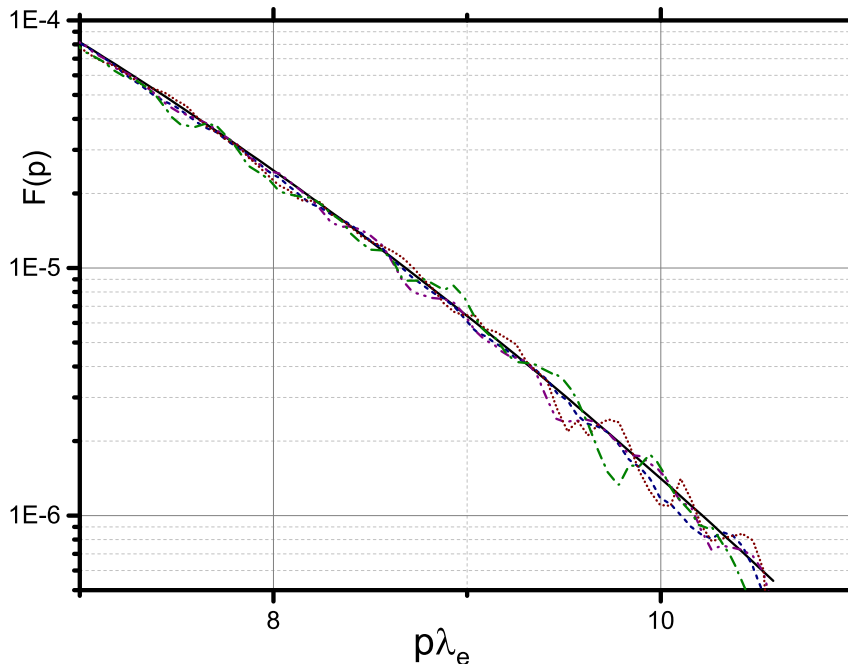
Figure 4: The same as in figure 3 but at high values of $p\lambda_e$ (in units of $\hbar$).

Note that the distribution functions are normalized to unit area under the curves. In logarithmic scale it may be difficult to see that, however the normalization is correct.

Momentum distribution functions for protonic component are presented in figures 3 and 4. The black solid line shows the maxwellian distribution, the other lines refer to the conditions mentioned above. Note that the units of momentum are $p\lambda_p^3$. All distributions are maxwellian under given parameters. The reason is that de Broglie wavelength of proton is much shorter than electronic one—$\lambda_p \approx 0.02\lambda_e$; under given conditions the protonic component is quite classical although the electronic one is essentially a quantum system.

Note that exchange corrections to electronic momentum distributions at $n_e\lambda = 0.3$ are quite significant. However they affect only the mean part of distribution making it Fermi instead of Maxwell. Quantum tales are results of dynamical scattering effect not depending on exchange.

4 CONCLUSIONS

In this paper formalism proposed and developed in [25, 26] is applied to non-degenerate hydrogen plasma. Path integral representation of Wigner function in harmonic approximation was used for studying of two-component Coulomb system. Problem of Coulomb singularity was overcome by using of Kelbg pseudopotential, which in path integral representation gives precise result. Suitable Monte-Carlo method was developed and embedded in software. Momentum distribution functions of non-degenerate hydrogen plasma with coupling strength Γ from 0.4 to

1.2 was calculated. Protons are maxwellian under considered conditions. On the contrary, electronic distribution functions have "quantum tails" at high momenta, that agrees qualitatively with theoretical predictions of [4]. In further papers we plan to compare our results with theoretical predictions quantitatively and improve precision of our numerical method.

The paper is based on the proceedings of the XXXII International Conference on Interaction of Intense Energy Fluxes with Matter, which was held in Elbrus settlement, in the Kabardino-Balkar Republic of the Russian Federation, from March 1 to 6, 2017.

REFERENCES

[1] V. M. Galitskii and V. V. Yakimets, "Particle relaxation in a Maxwell gas", *J. Exp. Theor. Phys.* **51**, 957 (1966).

[2] A. N. Starostin, A. B. Mironov, N. L. Aleksandrov, N. J. Fischc, and R. M. Kulsrudc, "Quantum corrections to the distribution function of particles over momentum in dense media", *Phys. A* **305**, 287–296 (2002).

[3] A. V. Emelianov, A. V. Eremin, Yu. V. Petrushevich, E. E. Sivkova, A. N. Starostin, M. D. Taran, and V. E. Fortov, "Quantum effects in the kinetics of the initiation of detonation condensation waves", *JETP Lett.* **94**, 530–534 (2011).

[4] A. V. Eletskii, A. N. Starostin, and M. D. Taran, "Quantum corrections to the equilibrium rate constants of inelastic processes", *Usp. Fiz. Nauk* **48**, 281–294 (2005).

[5] I. V. Kochetov, A. P. Napartovich, Yu. V. Petrushevich, A. N. Starostin, and M. D. Taran, "Calculation of thermal ignition time of hydrogen–air mixtures taking into account quantum corrections", *High Temp.* **54**, 563–568 (2016).

[6] R. Feynmann and A. Hibbs, *Quantum Mechanics and Path Integrals*, Moscow: Mir, (1968).

[7] V. S. Filinov, V. E. Fortov, M. Bonitz, and P. R. Levashov, "Phase transition in strongly degenerate hydrogen plasma", *JETP Lett.* **74**, 384 (2001).

[8] E. W. Brown, B. K. Clark, J. L. DuBois, and D. M. Ceperley, "Path-integral Monte Carlo simulation of the warm dense homogeneous electron gas", *Phys. Rev. Lett.* **110**, 146405 (2013).

[9] S. Groth, T. Schoof, T. Dornheim, and M. Bonitz, "Ab initio quantum Monte Carlo simulations of the uniform electron gas without fixed nodes", *Phys. Rev. B* **93**, 085102 (2016).

[10] T. Dornheim, S. Groth, T. Schoof, C. Hann, and M. Bonitz, "Ab initio quantum Monte Carlo simulations of the uniform electron gas without fixed nodes II: Unpolarized case", *Phys. Rev. B* **93**, 205134 (2016).

[11] V. S. Filinov, H. Fehske, M. Bonitz, V. E. Fortov, and P. R. Levashov, "Correlation effects in partially ionized mass asymmetric electron–hole plasmas", *Phys. Rev. E* **75**, 036401 (2007).

[12] D. M. Ceperley, "Path integrals in the theory of condensed helium", *Rev. Mod. Phys.* **67**(2), 279 (1995).

[13] T. Dornheim, A. Filinov, and M. Bonitz, "Superfluidity of trapped quantum systems in two and three dimensions", *Phys. Rev. B* **91**, 054503 (2015).

[14] T. Dornheim, D. Groth, A. Filinov, and M. Bonitz, "Permutation blocking path integral Monte Carlo: A highly efficient approach to the simulation of strongly degenerate non-ideal fermions", *New J. Phys.* **17**, 073017 (2015).

[15] V. S. Filinov, M. Bonitz, Yu. B. Ivanov, E. M. Ilgenfritz, and V. E. Fortov, "Color path integral equation of state of the quark–gluon plasma at nonzero chemical potential", *Plasma Phys. Controlled Fusion* **57**, 0440041 (2015).

[16] V. S. Filinov, Yu. B. Ivanov, M. Bonitz, V. E. Fortov, and P. R. Levashov, "Color path-integral Monte Carlo simulations of quark–gluon plasma", *Phys. Lett. A* **376**, 1096–1101 (2012).

[17] V. S. Filinov, Yu. B. Ivanov, M. Bonitz, V. E. Fortov, and P. R. Levashov, "Color path-integral Monte Carlo simulations of quark–gluon plasma: Thermodynamic and transport properties", *Phys. Rev. C* **87**, 035207 (2013).

[18] L. Shifren and D. Ferry, "Particle Monte Carlo simulation of Wigner function tunneling", *Phys. Lett. A* **285**, 217–221 (2001).

[19] L. Shifren and D. Ferry, "A Wigner function based ensemble Monte Carlo approach for accurate incorporation of quantum effects in device simulation", *J. Comput. Electron.* **1**, 55–58 (2002).

[20] L. Shifren and D. Ferry, "Wigner function quantum Monte Carlo", *Phys. B (Amsterdam, Neth.)* **314**, 72–75 (2002).

[21] D. Querlioz and P. Dollfus, *The Wigner Monte Carlo Method for Nanoelectronic Devices—A Particle Description of Quantum Transport and Decoherence*, ISTE-Wiley, (2010).

[22] J. M. Sellier, M. Nedjalkov, I. Dimov, and S. Selberherr, "A benchmark study of the Wigner Monte-Carlo method", *Monte Carlo Methods and Applications* **20**, 43–51 (2014).

[23] J. M. Sellier and I. Dimov, "On the simulation of indistinguishable fermions in the many-body Wigner formalism", *J. Comput. Phys.* **280**, 287–294 (2015).

[24] A. S. Larkin and V. S. Filinov, "Wigner's pseudo-particle relativistic dynamics in external potential field", *Phys. Lett. A* **378**, 1876–1882 (2014).

[25] A. S. Larkin, V. S. Filinov, and V. E. Fortov, "Path integral representation of the Wigner function in canonical ensemble", *Contrib. Plasma Phys.* **56**, 151–360 (2016).

[26] A. S. Larkin and V. S. Filinov, "Phase space path integral representation for Wigner function", *Journal of Applied Mathematics and Physics* **5**, 392–411 (2017).

[27] V. I. Tatarskiy, "Wigner representation of quantum mechanics", *Usp. Fiz. Nauk* **139**, 587–619 (1983).

[28] V. M. Zamalin and G. E. Norman, "The Monte-Carlo method in Feynman's formulation of quantum statistics", *USSR Comput. Math. Math. Phys* **13**, 408–420 (1973).

[29] A. V. Filinov, M. Bonitz, and W. Ebeling, "Improved Kelbg potential for correlated Coulomb systems", *J. Phys. A: Math. Gen.* **36**, 5957 (2003).